contribute to the miscibility of a homopolymer containing i segments with a copolymer containing j and k segments. Miscibility is aided by negative χ_{ij} and χ_{jk} of course, but also by a *positive* χ_{jk}. The importance of the latter is best comprehended by comparing the signs and magnitudes of the three terms in eq 4 at the critical point of certain of the binary blends. The three terms are calculated and entered in Table III for each of the four blends in which $i \neq j$ or k. The first and second terms in (4) arise from the interaction *between* the polymers, and the third term arises from the interaction of the j and k units *within* the copolymer. Because the third term is subtracted in (4), it contributes favorably to χ_{AB} (i.e., negatively) only when χ_{jk} is *positive*. In Table III the jk term for (3) is tabulated as a percentage of the total of the terms in (4) that favor mixing; the calculation of these terms is done at $\bar{x} = \bar{x}_c$. The point of this tabulation is to show that internal copolymer segmental "repulsion" can often be the dominant term favoring the mixing of a homopolymer and a copolymer. ("Repulsion" is used in a relative sense here; i.e., $\Delta\omega_{jk}$ is positive.) It suggests, in the extreme, that polymer systems exist in which none of the segment–segment χ's are negative yet in which miscibility occurs. This is most likely to be the case when the j and k segments differ greatly in polar character (as is the case with butadiene and acrylonitrile) and the i segment has an intermediate character (as is probably the case, for example, with vinyl chloride or methyl methacrylate); thus copolymer internal repulsion could account for the miscibility of poly(vinyl chloride) with, e.g., butadiene–acrylonitrile copolymers of intermediate compositions.[1]

Acknowledgment. We thank S. Y. Hobbs and V. H. Watkins for providing the scanning electron micrographs, P. E. Donahue and E. A. Williams for the nuclear magnetic resonance analysis, and D. M. White and J. Verbicki for guidance regarding the brominations.

Registry No. PS, 9003-53-6; PXE (SRU), 24938-67-8; 2,6-dimethylphenol homopolymer, 25134-01-4.

References and Notes

(1) Krause, S. In "Polymer Blends"; Paul, D. R., Newman, S., Eds.; Academic Press: New York, 1978; Vol. 1, Chapter 2.
(2) Nishi, T.; Wang, T. T.; Kwei, T. K. *Macromolecules* **1975**, *8*, 227.
(3) Karasz, F. E.; MacKnight, W. J. *Pure Appl. Chem.* **1980**, *52*, 409.
(4) Doube, C. P.; Walsh, D. J. *Polymer* **1979**, *20*, 1115.
(5) Walsh, D. J.; McKeown, J. G. *Polymer* **1980**, *21*, 1330, 1335.
(6) Roerdink, E.; Challa, G. *Polymer* **1980**, *21*, 1161.
(7) Sanchez, I. In "Polymer Blends"; Paul, D. R., Newman, S., Eds.; Academic Press: New York, 1978; Vol. 1, Chapter 3.
(8) White, D. M.; Orlando, C. M. In "Polyethers"; American Chemical Society: Washington, D.C., 1975; ACS Symp. Ser. No. 6.
(9) Stoelting, J.; Karasz, F. E.; MacKnight, W. J. *Polym. Eng. Sci.* **1970**, *10*, 133.
(10) Weeks, N. E.; Karasz, F. E.; MacKnight, W. J. *J. Appl. Phys.* **1977**, *48*, 4068.
(11) de Gennes, P.-G. "Scaling Concepts in Polymer Physics"; Cornell University Press: Ithaca (NY), London, 1979; p 106.
(12) "The Scientific Papers of J. Willard Gibbs"; Dover: London, 1961; Vol. 1, p 132.
(13) Alexandrovich, P. S. Doctoral Dissertation, University of Massachusetts, 1978.
(14) Rayn, C. L. Doctoral Dissertation, University of Massachusetts, 1979.

Dynamical Aspects of Phase Separation in Polymer Blends

Harold L. Snyder* and Paul Meakin

Central Research and Development Department,† E. I. du Pont de Nemours and Company, Experimental Station, Wilmington, Delaware 19898

Shymon Reich

Department of Plastics Research, Weizmann Institute of Science, Rehovot, Israel.
Received July 8, 1982

ABSTRACT: We have investigated the time development of structure in polystyrene/poly(vinyl methyl ether) blends using conventional light scattering techniques. We show that by utilizing the light scattering invariant and the angular dependence of scattering, one may quantitatively describe the early stages of phase separation within the framework of the linearized Cahn–Hilliard expression. By extrapolating the measured diffusion constant to where it undergoes a sign change, one may also determine the spinodal curve from this procedure.

Introduction

Although phase separation is a dynamical process, previous studies concerned with phase separation in polymer blends have concentrated on determining equilibrium properties, i.e., the phase diagram. van Aartsen[1,2] combined the Flory–Huggins free energy expression and Cahn–Hilliard equations to estimate the effect of spinodal decomposition in polymer/small-molecule systems and proposed an empirical method to define the spinodal temperature by monitoring the total isothermal light scattering intensity as a function of time. Others[3,4] have applied the Ornstein–Zernike–Debye theory to determine the spinodal curve. This procedure involves extrapolating light scattering as a result of density fluctuations to zero angle at a series of temperatures and extrapolating the temperature dependence of the zero-angle intensity to the temperature at which the scattering becomes discontinuous. All measurements are taken in the one-phase region to avoid complications caused by critical opalescence.[5] The utility of this procedure was illustrated in work performed on the polystyrene/cyclohexane system.[3,4] Goldsbrough et al. have experimentally extended Scholte's procedure by applying pulse induced scattering (PICS) techniques to determine the spinodal curve.[6] The PICS method is based on the assumption that it is possible by means of a rapid "thermal pulse" to jump into the metastable region, measure scattering as a result of fluctuations, and return to the one-phase region before appreciable phase separation has occurred. Analysis of PICS data is identical with Scholte's original procedure; however, the spinodal curve is determined via a shortened extrapolation length. The thermodynamic understanding of polymer blend phase diagrams has been advanced by the theoretical treatments

† Contribution No. 3072.

0024-9297/83/2216-0757$01.50/0

of Patterson,[27] McMaster,[7] and Koningsveld,[8] who applied a modified equation of state approach to examine the thermodynamic origins of miscibility and lower critical solution temperature (LCST) behavior and to calculate spinodal and binodal curves. However, except for a pulsed NMR experiment[9] and theoretical work by Pincus[10] and de Gennes,[11] there has been very little experimental or theoretical effort directed at understanding the dynamical aspects of phase separation in polymer blends. Dynamical studies are particularly important if one wishes to obtain quantitative information concerning the mechanism of phase separation.

The linearized Cahn–Hilliard[12-14] equations predict that two distinct phase separation mechanisms are possible. If the system is unstable toward infinitesimal concentration fluctuations (i.e., $\partial^2 f/\partial c^2 < 0$), then phase separation occurs via spinodal decomposition, which is best characterized in reciprocal space by an exponential growth of a single scattering peak. This is the result of a spatially periodic composition distribution which is induced by the dynamics of the phase separation process. Behavior similar to this has been observed in metallic alloys, glasses, and binary liquids.[13,14,28] However, in the late stages the scattering peak shifted to smaller angles, and there was deviation from the expected exponential growth law.[14] If the system is stable to infinitesimal concentration fluctuations (i.e., $\partial^2 f/\partial c^2 > 0$), then the Cahn–Hilliard treatment assumes that phase separation proceeds in the metastable region by conventional nucleation and growth mechanisms. Langer[15] has included thermal fluctuations in his treatment and has found results that are in qualitative agreement with some aspects of the Cahn–Hilliard treatment but differ in that coarsening processes are allowed and the time-dependent scattering is no longer necessarily exponential. Further, Langer notes that thermal fluctuations remove the discrete boundary between the spinodal and nucleation mechanisms. Simulations applying the kinetic Ising model, which include only nearest-neighbor interactions, do not show an exponential growth in scattering intensity even during the earliest stages of the phase separation process.[29-31] However, in theoretical treatments that allow for long-range interactions such as observed in a van der Waals[18] or Lennard-Jones[17] fluid, exponential growth is observed in the early stages of phase separation. It has been suggested that long-range interactions play a critical role in producing early exponential behavior. However, the conditions under which Cahn–Hilliard behavior is expected are still an open question.

We have undertaken a study to investigate the dynamics of phase separation in polymer blends. In particular, we will discuss the applicability of the Cahn–Hilliard formalism. We will also show that by assuming modified Flory–Huggins behavior, it is sufficient to monitor the total forward light scattering and the angular dependence of that scattering to determine the temperature and compositional dependence of the constants that characterize the Cahn–Hilliard spinodal decomposition processes. Further, we can directly measure the temperature dependence of an effective diffusion constant within the spinodal region and hence determine the spinodal/binodal curve. To demonstrate the application of the procedure, we investigated the polystyrene/poly(vinyl methyl ether) (PS/PVME) blend, which has been investigated in a number of previous studies.[19-26]

Experimental Section

The polystyrene and poly(vinyl methyl ether) used in this study were obtained from Polysciences, Inc. The polymer characteristics as analyzed by GPC are given in Table I.

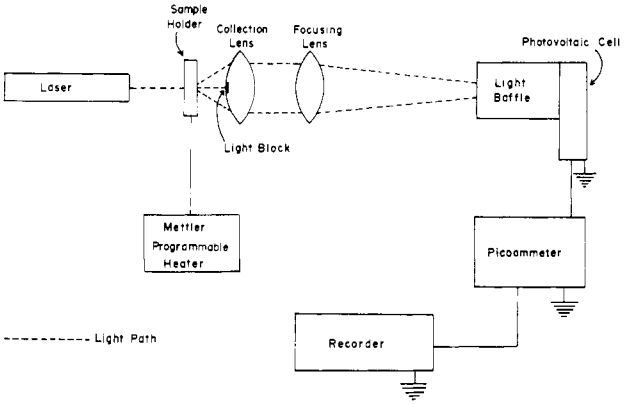

Figure 1. Experimental apparatus.

Table I
Characterization of Polymer Samples

polymer	M_n	M_w	M_w/M_n	M_z	M_z/M_w
PS	15 000	60 000	4	150 000	2.5
PVME	35 900	62 700	1.75	96 500	1.53

Thin films were prepared by mechanically dip coating glass slides into a toluene solution which contained 10% by weight polymer. The coating procedure was carried out in a nitrogen atmosphere, and excess solvent was eliminated by annealing slides at 80 °C in a vacuum oven for 48 h. Davis et al.[21] have shown that this procedure should be sufficient to remove any structural effects resulting from solution casting. We found this procedure resulted in homogeneous films that were 2–10 μm thick. If the film thickness was greater than about 0.5 μm, the light scattering characteristics of the early stages of phase separation was found to be independent of thickness. In previous work it was shown that the position of the binodal curve was independent of thickness if the film thickness was greater than 0.5 μm.[26] The film thickness used in experiments reported here was 3–4 μm.

Light scattering measurements were performed on an apparatus similar to that shown in Figure 1. The light source was a Liconix He/Cd 4416-Å laser, attenuated to produce a power of 5 μW. The sample was placed in a programmable heating stage that could be heated at 10, 2, or 1 °C/min or could be operated in an isothermal mode. In "isothermal" experiments, preheated homogeneous films underwent a rapid temperature jump to the isothermal setting. The total forward light scattering was collected with optics and focused onto a photovoltaic cell whose output was amplified and recorded. The linearity of the measured scattered intensity is estimated to be ±1% based on manufacturer-supplied operating data and specification.

It was also possible, using a slight modification, to determine the angular dependence of the peak scattering intensity. As a result of the development of periodic modulations in the refractive index, a broadened Fraunhofer diffraction ring was observed (Figure 2). The radius of this ring provides a direct measure of the characteristic dimension, d_m, associated with concentration modulations:

$$d_m \simeq \lambda/[2n \sin(\theta/2)] \quad (1)$$

λ is the wavelength of light and θ is the angle subtended by the collapsing ring.

Analysis of Scattering Data

The light scattering from an isotropic two-phase system has been investigated by Stein et al.,[25] and it was shown that in the Rayleigh limit the measured light scattering invariant or total integrated intensity was independent of the size and shape of the scattering elements and is given by

$$Q_{SAL} = P(\lambda)\int R(\beta)\beta^2 \, d\beta = \frac{32\pi^6}{\lambda^4}\langle\eta^2\rangle P(\lambda) \quad (2)$$

where $R(\beta)$ is the Rayleigh factor, β is the magnitude of

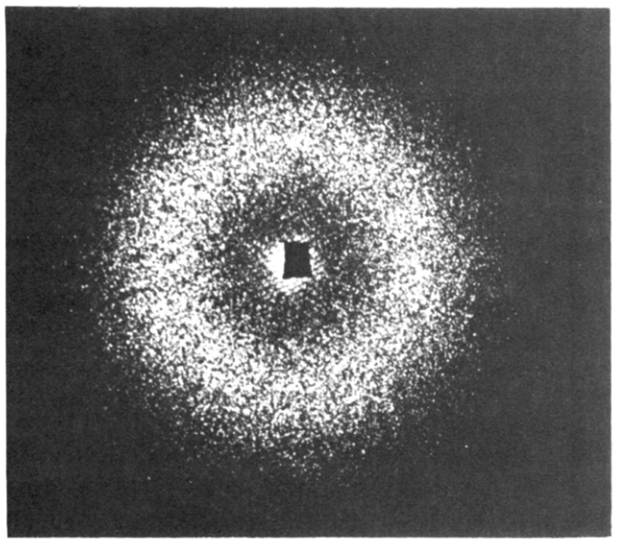

Figure 2. Observed scattering pattern resulting from phase separation in polymer blends.

the scattering vector, $P(\lambda)$ is the apparatus efficiency, and $\langle\eta^2\rangle$ is the mean-square average of all fluctuations related to the polarizability. In the two-phase model, $\langle\eta^2\rangle$ is given by

$$\langle\eta^2\rangle = \phi_1\phi_2(\alpha_1 - \alpha_2)^2 \tag{3}$$

where ϕ_1 and ϕ_2 are volume fractions of the two phases, and $(\alpha_1 - \alpha_2)^2$ is the square of the difference of the respective polarizabilities, which may be related to the differences in the index of refraction of the two phases, $\Delta N = N_1 - N_2$, and the average index of refraction, $\bar{N}_0$, via the Lorentz–Lorenz equation.

$$\alpha_1 - \alpha_2 = \frac{9\bar{N}_0(N_1 - N_2)}{2\pi(\bar{N}_0^2 + 2)^2} \tag{4}$$

Assuming the difference in refractive index is proportional to the concentration difference, $\Delta N = \Lambda\Delta c$, we obtain

$$Q_{SAL} = \frac{648\pi^4}{\lambda^4}\frac{\bar{N}_0^2}{(\bar{N}_0^2 + 2)^4}[\Lambda\Delta c]^2P(\lambda)\phi_1\phi_2 \tag{5}$$

This implies that by monitoring the total forward light scattering as a function of time, we may directly measure the time-dependent growth of Δc, and the Cahn–Hilliard model may be examined by using the results of eq 5.

By recognizing the contribution of nonhomogeneous effects, Cahn and Hilliard[12-14] wrote an expression to describe the change in concentration as a function of time during a spinodal process

$$\frac{\partial c}{\partial t} = M\left(\frac{\partial^2 f}{\partial c^2}\right)\nabla^2 c - 2MK\nabla^4 c + \text{nonlinear term} \tag{6}$$

where f is the free energy, c is the concentration, M is the diffusional mobility, and K has been termed the energy gradient coefficient parameter. If nonlinear terms are dropped, eq 6 has the following solution[14]

$$c - c_0 = \sum_\beta \exp[R(\beta)t][A(\beta)\cos(\beta r) + B(\beta)\sin(\beta r)] \tag{7}$$

where c is the phase composition, c_0 is the average composition before phase separation, β is the wavenumber of the sinusoidal composition fluctuations, t is the time variable, r is the position variable, and $R(\beta)$ (which may be thought of as a first-order rate constant describing the phase separation process) is given by

$$R(\beta) = -M\left(\frac{\partial^2 f}{\partial c^2}\right)\beta^2 - 2MK\beta^4 \tag{8}$$

Cahn[12] has shown that in his linearized theory only fluctuations with a wave vector, β, smaller than some critical value, β_c, will yield a positive growth rate and that all fluctuations with a larger wave vector than this value will decay with time. Further, $R(\beta)$ has a rather sharp maximum, $R(\beta_m)$, and we will assume that only fluctuations with a wave vector close to β_m contribute significantly to the phase separation process.

$$c - c_0 = \exp[R(\beta_m)t][A(\beta_m)\cos(\beta_m r) + B(\beta_m)\sin(\beta_m r)] \tag{9}$$

and

$$R(\beta_m) = -\tfrac{1}{2}\left(\frac{\partial^2 f}{\partial c^2}\right)\beta_m^2 M = -\tfrac{1}{2}\bar{D}\beta_m^2 \tag{10}$$

$\bar{D}$ is the effective or Cahn–Hilliard diffusion constant. Recognizing that $\Delta c = 2(c - c_0)$ and combining eq 5 and 9, we obtain

$$Q_{SAL} = \frac{2592\pi^4}{\lambda^4}\phi_1\phi_2\frac{\bar{N}_0^2}{(N_0^2 + 2)^2}\Lambda[\exp[R(\beta_m)t]^2] \times [A(\beta_m)\cos(\beta_m r) + B(\beta_m)\sin(\beta_m r)]^2P(\lambda) \tag{11}$$

or the time-dependent behavior may be written as

$$Q_{SAL}(t) \propto e^{2R(\beta_m)t} \tag{11a}$$

A plot of $\ln (Q_{SAL})^{1/2}$ vs. time should yield a straight line whose slope is equal to $R(\beta_m)$. By measuring the time dependence of $Q_{SAL}(t)$ at several temperatures within the spinodal, we may obtain the temperature dependence of $R(\beta_m)$. Further, if β_m is known, we can also measure the temperature dependence of $\bar{D}$ using eq 10, and β_m is determined from the angular dependence of light scattering and eq 1.

Equation 5 implies that light scattering is a function of only concentration fluctuations and ignores contributions as the result of the average square of the local fluctuation gradient, which Debye[5] has shown to be important near the critical point. This is a result of a pseudodiscontinuity in the isothermal compressibility that occurs near the critical point.

$$K_T \sim [(T - T_c)/T_c]^{-\gamma'} \qquad T < T_c \tag{12}$$

$$K_T \sim [(T - T_c)/T_c]^{-\gamma} \qquad T > T_c \tag{12a}$$

where K_T is the isothermal compressibility, T_c is the critical temperature, and γ and γ' are critical exponents. Equations 12 illustrate that on either side of T_c similar behavior is observed, and if $|T - T_c|$ is large, the Debye scattering correction is small. Scattering may be performed in either the one-phase or two-phase region (Figure 3) as long as $|T - T_c|$ is large and the phase separation process is slow compared to temperature equilibration time. This should be true if $|T - T_c| > 1$ °C.[5]

Results

The cloud-point curve in Figure 3 was constructed by using data from isothermal experiments. If the development of scattering intensity was not observed after 2 h at a specified temperature, the sample was considered to be below the polymer blend cloud-point temperature. The observed lower critical solution temperature cloud-point curve is reliable to ±0.5 °C and is consistent with the results of previous workers.[20]

Further, consistent with the work of Bank et al.,[22,23] a single (but broadened) glass transition was observed in the one-phase region while the individual PS and PVME glass

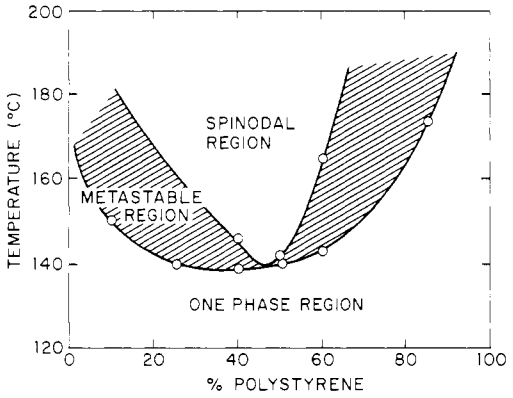

Figure 3. Phase diagram determined for the polystyrene/poly(vinyl methly ether) system. The binodal was determined by using cloud point measurements and the behavior of the glass transition. The spinodal curve was determined by extrapolating the diffusion constant to where a change in sign takes place.

transitions were observed in the two-phase region. The T_g of the PS/PVME 60/40 composition was 30 °C, and the T_g of the 85/15 composition was 53 °C. As found by Davis et al.,[21] a phase-separated sample could be rehomogenized by annealing below T_g. It was also observed that the position and shape of the cloud point were sensitive to heating rate and that the scan rate dependence of the cloud point was more pronounced in regions where the metastable gap was large, resulting in a more sharply dipped cloud point curve than observed in isothermal experiments (Figure 3).

The phase separation process as observed in PS/PVME mixtures may be categorized into three broad areas: early stage, breakup stage, and coalescence and growth stage. The morphology of the early stages is dominated by the appearance and growth of a very regular intertwined structure. As the concentration gradient between the two phases becomes critical, this structure breaks up to form small droplets which grow. This report will discuss only the initial stages of the phase separation process.

The isothermal scattering results from phase separation of a 50/50, 40/60, and 60/40 mixture of PS/PVME were monitored as a function of time, and the initial stages of phase separation were evaluated by utilizing eq 1, 5, and 11. The linearized Cahn–Hilliard expression predicts that during the early stages of phase separation an exponential growth in the scattering intensity should be observed. The scattering curves in Figure 4A–C demonstrate that this exponential behavior is observed. However, it should be stressed that the exponential behavior was observed for only the first 5–10% of the phase separation which occurred before the breakup process became dominant. Cahn and Hilliard also predict that a sinusoidal spatial modulation will occur during the early stages of the phase separation process. Evidence for this type of behavior was observed with the development of a characteristic Fraunhofer diffraction ring (Figure 2). Within the resolution of our experiment, β_m, as determined from the diffraction ring, was at most a very slowly varying function of time during the early stages of phase separation, and the results of our experiment are consistent with the Cahn–Hilliard prediction during the early stages of the phase separation process. However, as expected, the later stages of the phase separation clearly have major deviations from the Cahn–Hilliard model.

From the slope of ln $Q_{SAL}^{1/2}(t)$ vs. time (Figure 4) and the radius of the scattering ring, we determined the temperature dependence of the Cahn–Hilliard diffusion constant for the 40/60, 50/50, and 60/40 PS/PVME blends

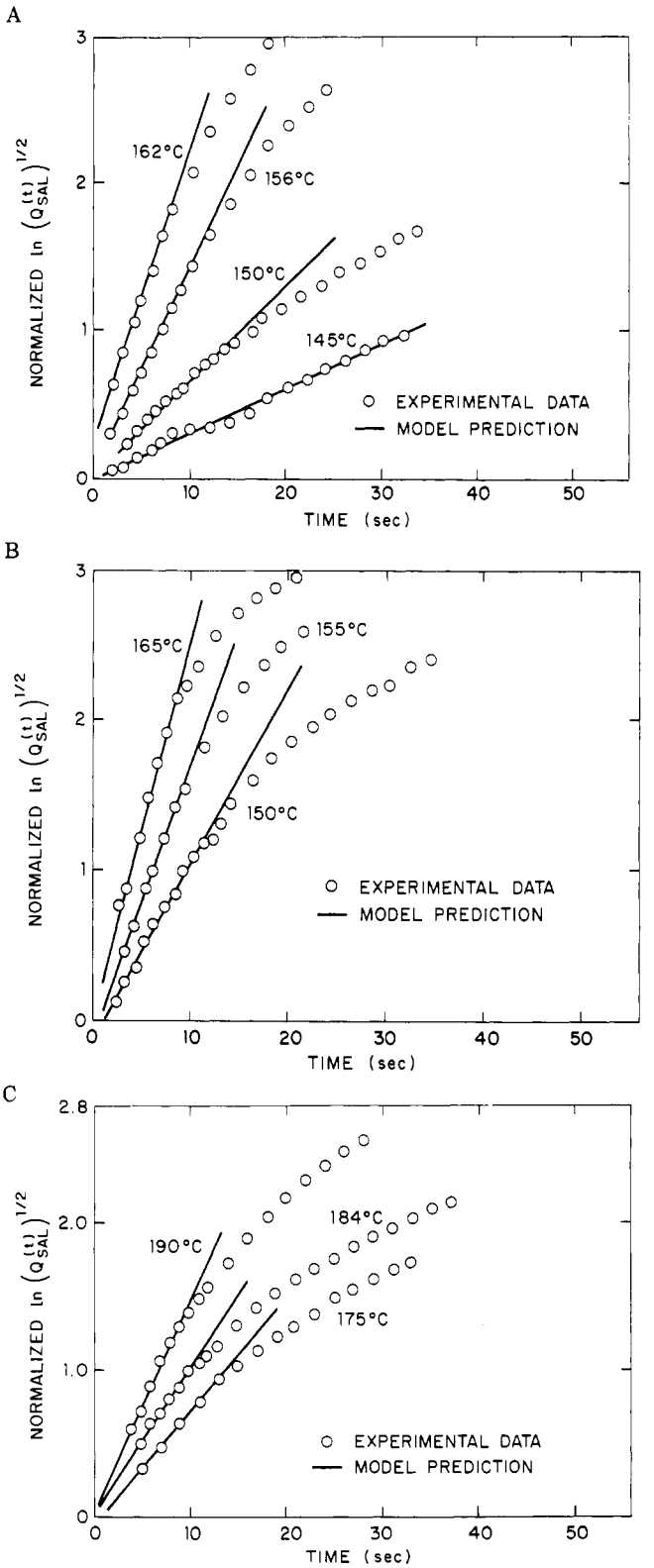

Figure 4. Scattering curves obtained during the phase separation process. The weight composition for each curve was (A) 50/50 PS/PVME, (B) 40/60 PS/PVME, and (C) 60/40 PS/PVME.

(Figure 5). The temperature dependence of the Cahn–Hilliard diffusion constant was linear. The spinodal curve (Figure 3) was determined by extrapolating the diffusion constant to where it changed sign (Figure 5).

Discussion

Cahn has shown that within the unstable region the diffusion constant is given by

$$D = M(\partial^2 f/\partial c^2) \tag{13}$$

Table II
Spinodal Constants

composition, % PS	temp, °C	T_s, °C	$\beta_m \times 10^{-4}$, cm^{-1}	$\overline{R(\beta_m)}$, s^{-1}	$-10^{11}D_2$, cm s^{-1}	$-(\partial^2 f/\partial c^2)$, cal cm^{-3} (PVME)	$M \times 10^{10}$	$K \times 10^{10}$
40	150	147	3.00	0.102 ± 0.04	22.70 ± 8	0.64	3.55	1.78
40	155	147	2.47	0.157 ± 0.02	51.46 ± 9	2.79	1.84	11.40
40	160	147	2.27	0.20 ± 0.02	77.6 ± 10	2.79	2.78	13.52
40	165	147	2.01	0.24 ± 0.02	118.9 ± 12	3.87	3.07	23.94
50	145	142	4.26	0.03 ± 0.003	3.3 ± 0.8	0.67	0.49	0.911
50	147	142	4.26	0.047 ± 0.01	5.2 ± 1.2	1.11	0.47	1.54
50	149	142	3.94	0.063 ± 0.003	8.1 ± 1.0	1.55	0.52	2.48
50	150	142	4.26	0.075 ± 0.002	8.3 ± 1.2	1.78	0.47	2.48
50	153	142	4.26	0.11 ± 0.02	12.1 ± 1.6	2.45	0.49	3.34
50	156	142	4.26	0.138 ± 0.02	15.2 ± 1.6	3.12	0.48	4.24
50	159	142	4.26	0.16 ± 0.02	17.6 ± 1.6	3.78	0.46	5.13
50	162	142	4.26	0.19 ± 0.03	20.8 ± 1.6	4.45	0.46	6.02
60	175	165	6.01	0.058 ± 0.02	3.2 ± 1	1.91	0.17	1.33
60	180	165	5.8	0.082 ± 0.02	4.87 ± 1	2.87	0.17	2.13
60	182	165	5.8	0.093 ± 0.02	5.29 ± 1	3.26	0.16	2.28
60	184	165	5.8	0.103 ± 0.02	6.12 ± 1	3.64	0.18	2.89
60	186	165	5.8	0.122 ± 0.02	7.25 ± 1	4.02	0.18	2.98
60	190	165	5.8	0.144 ± 0.02	8.56 ± 0.8	4.79	0.18	3.59

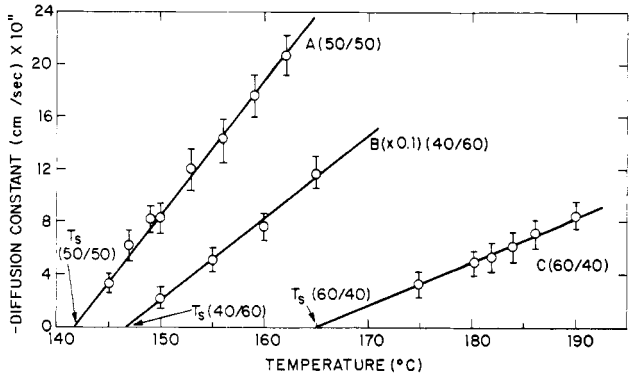

Figure 5. Temperature dependence of diffusion constant. The weight composition for each curve was (A) 50/50 PS/PVME, (B) 40/60 PS/PVME, and (C) 60/40 PS/PVME. The spinodal curve is given by the intercept on the temperature axis.

We will describe the free energy of the phase separation process using the familiar Flory–Huggins model as modified by de Gennes. The applicability of this model to phase separation processes has recently been discussed by several authors,[10,11] and the molar free energy of a polymer blend in the Flory–Huggins model is given by

$$f = RT\left[\frac{\phi_1}{v_1}\ln\phi_1 + \frac{\phi_2}{v_2}\ln\phi_2 - \frac{\phi_1\phi_2\chi}{v_1} + \frac{a^2}{36\phi_2(1-\phi_2)}(\nabla\phi_2)^2\right] \quad (14)$$

where ϕ_1 and ϕ_2 are the local concentrations of polymers 1 and 2, v_1 and v_2 are the molar volumes, Na^2 is the mean-square end-to-end distance, and χ is the mean field interaction, which is often given the form

$$\chi = A + BV/RT \quad (15)$$

where A and B are constants which are commonly assumed to be temperature independent. This assumption is reasonable over the limited temperature range probed in this experiment. The diffusion constant is proportional to the second derivative of the free energy with concentration; hence

$$\frac{\partial^2 f}{\partial\phi_2^2} = RT\left[\frac{1}{v_1\phi_1} + \frac{1}{v_2(1-\phi_1)} + \frac{2\chi}{v_1} + F(\phi_2)\right] \quad (16)$$

where $F(\phi)$ is a simple function of concentration. At the spinodal $\partial^2 f/\partial\phi_2^2 = 0$ and

$$\frac{1}{v_1\phi_1} + \frac{1}{v_2(1-\phi_1)} + F(\phi_2) = \frac{2\chi^s}{v_1} \quad (17)$$

where χ^s is the mean field interaction parameter at the spinodal temperature, and from this result

$$\partial^2 f/\partial\phi_1^2 = 2B[(T_s - T)/T_s] \quad (18)$$

$$D = 2BM[(T_s - T)/T_s] \quad (19)$$

Equation 19 is analogous to proposed scaling relationships for the diffusion constant, i.e.,[2,3]

$$D \propto [(T_s - T)/T_s]^{\gamma^*} \quad (20)$$

and γ^* has been measured for a number of small-molecule systems and was found to be about 0.66.[3] We observe that γ^* is nearly equal to 1, which is what is predicted by the linearized Flory–Huggins/Cahn–Hilliard model. This is in marked contrast to the exponential WLF behavior, which has been so successful in describing noncritical polymer diffusion. A value of 15.8 cal/cm^3 has been determined for B in the PS/PVME system.[9] This enables us to calculate the temperature and compositional dependence of all other Cahn–Hilliard parameters using eq 18 and the Cahn–Hilliard relationships[12-14]

$$R_m = M(\partial^2 f/\partial c^2)^2/8K \quad (21)$$

$$R_m = -\tfrac{1}{2}(\partial^2 f/\partial c^2)\beta_m^2 M \quad (22)$$

The results of these calculations are given in Table II and give a complete Cahn–Hilliard description of the early stages of the phase separation process. These results have been compared with the predictions of the de Gennes–Pincus[10,11] model for spinodal decomposition in polymer blends. Although the criteria presented in the model would suggest we are in a shallow-quench region, the results of our experiments are more consistent with the deep-quench predictions. In particular, we observe that the optimal growth rate scales linearly with temperature.

Conclusion

Using simple light scattering experiments, it is possible to probe the dynamics of the early stages of phase separation. Consistent with the Cahn–Hilliard model, an initial exponential growth in the scattering intensity is observed.

We have developed a new procedure by which one may measure diffusion constants and spinodal curves in polymer blends. Exponential growth in the concentration gradient $(c - c_0)$ was observed during the early stages of phase separation, after which time the Cahn–Hilliard expression becomes clearly inadequate. From the growth of the scattering intensity and the angular dependence of that scattering, it was possible to give a complete quantitative description of the early stages of polymer blend phase separation in the PS/PVME system.

References and Notes

(1) van Aartsen, J. J. *Eur. Polym. J.* **1970**, *6*, 919.
(2) van Aartsen, J. J. *Eur. Polym. J.* **1970**, *6*, 1105.
(3) Kuwshara, N.; Fenly, D. V.; Tamsky, M.; Chu, B. *J. Chem. Phys.* **1970**, *55*, 1140.
(4) Scholte, Th. G. *Eur. Polym. J.* **1970**, *6*, 1063.
(5) Debye, P. *J. Chem. Phys.* **1959**, *31*, 680.
(6) Goldsbrough, J. *Sci. Prog.* **1972**, *60*, 281.
(7) McMaster, L. P. *Macromolecules* **1973**, *6*, 760.
(8) Koningsveld, R.; Kleintjens, L. A.; Schoffelens, H. M. *Pure Appl. Chem.* **1974**, *39*, 1.
(9) Nishi, T.; Wang, T. T.; Kwei, T. K. *Macromolecules* **1975**, *8*, 227.
(10) Pincus, P. *J. Chem. Phys.* **1981**, *75*, 1996.
(11) de Gennes, P.-G. *J. Chem. Phys.* **1980**, *72*, 4756.
(12) Cahn, J. W. *J. Chem. Phys.* **1965**, *42*, 93.
(13) Hilliard, J. E. In "Phase Transformations". Seminar of the American Society for Metals, Oct 1968, p 497.
(14) Cahn, J. W. *Trans. Am. Inst. Min., Metall. Pet. Eng.* **1968**, *242*, 166.
(15) Langer, J. S. In "Fluctuations, Instabilities and Phase Transitions"; Riste, T., Ed.; Plenum Press: New York, 1975.
(16) Sur, A.; Lebowitz, J. L.; Marro, J.; Kalos, M. H. *Phys. Rev. B.* **1977**, *15*, 3014.
(17) Mruyik, M. R.; Abraham, F. F.; Pound, G. M. *J. Chem. Phys.* **1978**, *69*, 3462.
(18) Varea, C.; Robledo, A. *J. Chem. Phys.* **1981**, *75*, 5080.
(19) Kuwahara, N.; Ishiyawa, M.; Saeki, S.; Kaneka, M. *Rep. Prog. Polym. Phys. Jpn.* **1976**, *13*, 9.
(20) Nishi, T.; Kwei, T. K. *Polymer* **1976**, *16*, 285.
(21) Davis, D. D.; Kwei, T. K. *J. Polym. Sci., Polym. Phys. Ed.* **1980**, *18*, 2337.
(22) Bank, M.; Liffingwell, J.; Thies, C. *J. Polym. Sci., Polym. Phys. Ed.* **1972**, *10*, 1097.
(23) Bank, M.; Leffingwell, J.; Thies, C. *Macromolecules* **1971**, *4*, 43.
(24) Hourston, O. J.; Hughes, I. D. *Polymer* **1978**, *19*, 1181.
(25) Kobertstein, J.; Russell, T. P.; Stein, R. S. *J. Polym. Sci., Polym. Phys. Ed* **1979**, *17*, 1719.
(26) Reich, S.; Cohen, Y. *J. Polym. Sci., Polym. Phys. Ed.* **1981**, *19*, 1255.
(27) Patterson, D.; Robard, A. *Macromolecules*, **1978**, *11*, 690.
(28) Huang, J. S.; Goldberg, W. I.; Bjerkcas, A. W. *Phys. Rev. Lett.* **1974**, *32*, 921.
(29) Bortz, A. B.; Kalos, M. H.; Lebowitz, J. L.; Zendejas, M. A. *Phys. Rev. B* **1974**, *10*, 535.
(30) Sur, A.; Lebowitz, J. L.; Marro, J.; Kalos, M. H. *Phys. Rev. B* **1977**, *15*, 3014.
(31) Marro, J.; Bortz, A. B.; Kalos, M. H.; Lebowitz, J. L. *Phys. Rev. B* **1975**, *12*, 2000.

Melting Behavior of Crystalline/Compatible Polymer Blends: Poly(ϵ-caprolactone)/Poly(styrene-*co*-acrylonitrile)

Peter B. Rim and James P. Runt*

The Pennsylvania State University, Department of Materials Science and Engineering, Polymer Science Program, University Park, Pennsylvania 16802.

Received September 29, 1982

ABSTRACT: The crystallinity and melting of compatible poly(ϵ-caprolactone)/poly(styrene-*co*-acrylonitrile) (PCL/SAN) blends were monitored for samples prepared from both the melt and solution. The development of PCL crystallinity was observed to be dependent on both the blend composition and preparation technique. The glass transition temperature was observed to be a primary cause of the compositional dependence of crystallinity. Solution casting was found to be a technique capable of increasing crystallinity levels for some compositions. The melting behavior of the blends is rather complex. Solution-cast samples exhibited a single endotherm that decreased in temperature with increasing SAN concentration. Both thermodynamic and morphological effects are cited as possible causes of this behavior. Melt-crystallized samples exhibited dual-melting endotherms whose magnitudes vary with blend composition. The melting point of the lower temperature endotherm increased with increasing SAN concentration. A mechanism based on melting, recrystallization, and subsequent remelting is invoked to explain the behavior of the melt-crystallized specimens. Finally, problems encountered when calculating polymer–polymer interaction parameters directly from experimental melting data are discussed.

I. Introduction

Thermal analysis techniques such as differential thermal analysis (DTA) and differential scanning calorimetry (DSC) have been used frequently to study compatible polymer blends. The usefulness of these techniques can be multipurpose. Observation of glass transition temperatures (T_g) that are between those of the pure blend components is often cited as evidence of compatibility. For compatible blends in which one or more of the components are capable of crystallization (crystalline/compatible blends), thermal techniques are often used to monitor crystalline melting points as well as extents of crystallization.

As might be expected, T_g has been observed to be a major factor influencing the degree of crystallinity in crystalline/compatible blends.[1,2] For melt-crystallized specimens crystallization can proceed if the crystallization temperature (T_c) is between the blend equilibrium melting point ($T_m°$) amd T_g. However, work performed in our laboratory on poly(ϵ-caprolactone)/poly(styrene-*co*-acrylonitrile) (PCL/SAN) blends has shown that the common blend preparation technique of solution casting can lead to a modification of the temperature range over which crystallization occurs.[1] It was observed that crystallization could be induced in crystalline/compatible blends that are normally amorphous when prepared from the melt. This behavior is believed to result from a solvent-induced crystallization process. This previous study was performed on one composition (80% SAN/20% PCL) of the PCL/SAN blend system. One purpose of the

0024-9297/83/2216-0762$01.50/0